



Role of metal impurity in hydrogen diffusion from surface into bulk magnesium: A theoretical study



Zhao-Yi Wang^a, Yu-Jun Zhao^{a,b,*}

^a Department of Physics, South China University of Technology, Guangzhou, Guangdong 510640, China

^b Key laboratory of Advanced Energy Storage Materials of Guangdong Province, South China University of Technology, Guangzhou, Guangdong 510640, China

ARTICLE INFO

Article history:

Received 10 August 2017

Received in revised form 17 September 2017

Accepted 22 September 2017

Available online 25 September 2017

Communicated by R. Wu

Keywords:

First-principles study

Hydrogen diffusion

Magnesium

Metal impurity

ABSTRACT

We have systematically studied the role of four typical metal impurities (Ti, Nb, Al, and In) in the diffusion of hydrogen atoms into magnesium bulk by first-principles calculations. We find that Ti, Nb, and Al energetically prefer to substitute Mg atoms in the inner layers rather than the outmost layer, which In favors, with the consideration of H adsorption. The existence of the subsurface Ti or Nb atoms enhances hydrogen atom diffusion with respect to the pure Mg system, beneficial to the formation of H–Mg–H trilayer structure and its subsequent transition to Mg hydride. The doped Al or In atoms, however, provide no obvious help to the formation of MgH₂.

© 2017 Elsevier B.V. All rights reserved.

1. Introduction

The widely challenged energy crisis and environmental pollution are intensively associated with the large amounts carbon dioxide produced by limited fossil fuels [1], which could be replaced by many environment friendly energy sources, such as solar, wind, biomass energies etc. For the ultimate utilization of these renewable energies, especially in mobile industry, hydrogen energy is vital due to its high energy density and clean product, as well as easily transformed to various energy forms [2]. One of the key issues for the applications of hydrogen fuel cell technology is to find safe and efficient hydrogen storage materials. Hydrogen storage materials mainly include conventional metal hydride, chemical hydrides, complex hydrides, and sorbent systems [3], but the challenge remains for finding suitable hydrogen storage materials to satisfy U.S. Department of Energy (DOE) 2020 light-duty vehicle system targets [4], regardless of constant effort of decades.

On the basis of the high gravimetric hydrogen capacity of 7.7 wt% and high energy density of 9.9 MJ/kg [5], magnesium, a relative simple system with a low price as well, is a promising candidate for hydrogen storage materials of hydrogen fuel cells [6]. There are, however, still two serious limitations for the practical applications of magnesium hydride: high dehydrogenation tem-

perature and slow hydrogen sorption kinetics [7]. It should be pointed out that the hydrogenation of Mg occurs at a temperature as high as 350–400 °C under a hydrogen pressure of greater than 3 MPa [8]. In order to find feasible magnesium-based hydrogen storage materials, it is crucial to understand their hydrogenation process, which is often divided into several basic steps. The dissociation of hydrogen molecules, the diffusion of hydrogen atoms from surface into bulk, the formation of host metal solid solution dissolved with hydrogen, and finally the transition to metal hydride [9].

Vegge showed that the dissociation and recombination of hydrogen molecules was the rate-limiting processes in adsorption and desorption of hydrogen at the Mg (0001) surface [10]. It should be pointed out that earlier theoretical studies paid attention mostly to the effect of catalysts on the surface dissociation and adsorption of hydrogen. Several approaches have been proposed to overcome the dissociation barrier of hydrogen molecules: catalysts [11], steps [12], defects [13] and tensile strain [14]. We also studied the stability of TMs on Mg (0001) surface and their effects on hydrogen adsorption and found that a combined Ti and Nb co-doping is effective in promoting hydrogen dissociation and adsorption [15]. Dai et al. reported that Al can improve the dehydrogenation properties of MgH₂ system by weakening the interaction between Mg and hydrogen atoms [16]. Magnesium can form Mg–In solid solution alloys through mechanical alloying with indium. Mg (In) solid solution, which can be reversibly formed by

* Corresponding author at: South China University of Technology, Department of Physics, 381 Wushan Rd., Guangzhou, Guangdong 510640, China.

E-mail address: zhaoyj@scut.edu.cn (Y.-J. Zhao).

dehydrating from its hydrogenated produces, shows lowered reaction enthalpy compared with pure Mg [17].

Nevertheless, the diffusion of hydrogen from surface into bulk interstitial sites is an essential step to form magnesium hydride since the rate-limiting step will become the diffusion of hydrogen through the growing MgH₂ layer once MgH₂ nucleates [18]. Jiang et al. found a stable local H–Mg–H trilayer, a precursor state for Mg hydride [19]. Later on, our study revealed that the biaxial strain remarkably affects the structural stabilities of Mg–H system and found that the formation of the H–Mg–H trilayers is assisted by compressed strains while the following transition to Mg hydride would be helped by tensile strains [20]. We also studied the express penetration of hydrogen on Mg (10 $\bar{1}$ 3) along the close-packed-planes, indicating the crucial role of hydrogen diffusion in Mg hydrogenation [21]. With the repetition and stack of H–Mg–H trilayer structure, the formation of MgH₂ will be favorable. Xin et al. studied the effects of subsurface Mg vacancy on hydrogen trapping property and diffusion of hydrogen, concluding that the diffusion route and barrier of hydrogen atom are hardly affected by the subsurface vacancies [22].

In this paper, we select four typical metal impurities (Ti, Nb, Al, and In) with consideration of their interaction strength with H atoms and have systematically investigated the diffusion of adsorbed hydrogen atoms from surface into bulk magnesium. We reveal that the doped Ti or Nb enhances hydrogen atom diffusion and promotes formation of H–Mg–H trilayer structure, while the doped Al/In does not.

2. Computational method

All our calculations were performed with Vienna Ab initio Simulation Package (VASP) based on the Density Functional Theory (DFT) [23,24]. We used projector augmented wave (PAW) potentials [25,26] to describe the electron–ion interactions, and the generalized gradient approximation (GGA-PBE) [27] was used for the calculation of the exchange–correlation functional. For all calculation, the electron wave function was expanded using plane waves with an energy cutoff of 400 eV. For all of the relaxations, the energy difference of 10^{−4} eV was set as the convergence criterion between successive ionic steps and the forces on each atom were minimized up to 0.01 eV/Å [28].

The optimized lattice constants of bulk Mg of hexagonal structure were $a = 3.19$ Å and $c = 5.21$ Å, and the cohesive energy (E_{coh}) was 1.50 eV/atom in our calculations, in good agreement with the experimental values [29] ($a = 3.21$ Å, $c = 5.21$ Å, and $E_{\text{coh}} = 1.51$ eV/atom) and previous theoretical results [30]. The Mg (0001) surface with four catalysts doped for only single hydrogen adsorption and diffusion was modeled using a 3×3 surface unit cell with six atomic layers. The Brillouin zone of the Mg (0001) surfaces were sampled with a $5 \times 5 \times 1$ k-point mesh following the Monkhorst–Pack scheme [31]. The vacuum space was set to 15 Å to guarantee a sufficient separation between the periodic images along the z direction. Hydrogen and Mg atoms in the top four layers were fully relaxed in the calculations, whereas the bottom two layers were fixed at their bulk configurations. Convergence tests indicated that the cutoff energy and k-point sampling were sufficient to have the energy converged within 1 meV per atom.

The minimum energy path (MEP) for the diffusion and the corresponding diffusion barrier were determined using the climbing image nudged elastic band (CI-NEB) method [32]. For each diffusion path, we selected at least seven images to optimize simultaneously to get the MEP and the migration barrier. The spring constant of 5.0 eV/Å² was used for all diffusion barrier calculations and the force convergence criteria for each atom of images was set to 0.03 eV/Å.

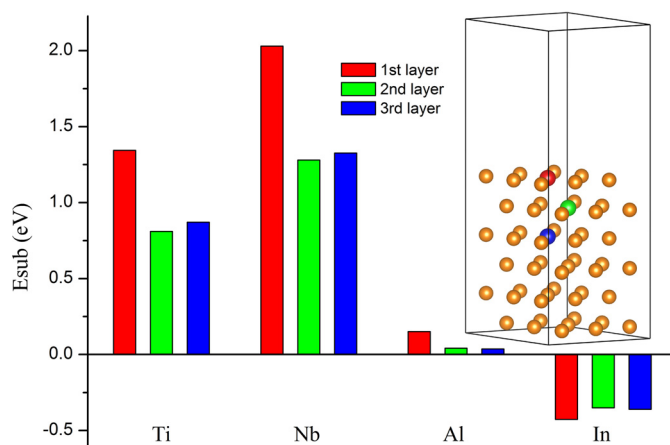


Fig. 1. (Color online.) The substitutional energy of four typical metal impurities (Ti, Nb, Al, and In). The red, green, and blue bar graph represent metal impurities doped in the first, second, and third layers, respectively. The inset graph in the right panel shows the structure of our Mg (0001) surface model.

3. Results and discussions

3.1. Substitutional energy and site preference

First, we have studied the stability of four typical metal impurities substitutions in different layers of Mg (0001). The interstitial sites are not considered for the impurities since Banerjee et al. has reported that these sites are not favored energetically [33]. The substitutional energy for metal impurities doped Mg (0001) surface is defined as:

$$E_{\text{sub}} = E_{\text{M/Mg}(0001)} + E_{\text{Mg}} - E_{\text{M}} - E_{\text{Mg}(0001)}, \quad (1)$$

where $E_{\text{M/Mg}(0001)}$ is the energy of the metal impurities substituted Mg surface, E_{Mg} and E_{M} is the energy of the Mg and metal impurities in the corresponding bulk structures, and $E_{\text{Mg}(0001)}$ is the energy of a clean Mg surface. By definition, a negative E_{sub} value implies that the metal impurities will not segregate from bulk Mg. The calculated E_{sub} values for various metal impurities at different layers of the Mg surfaces are illustrated in Fig. 1.

The negative substitutional energy of In indicate that In is miscible in bulk Mg. This is consistent with the fact that Mg and In will form Mg–In solid solution alloys by mechanical alloying. It is clear that the substitutional energy of Al is a rather small although positive, in line with the fact that Mg–Al compound can also form in experiment and Al can also dissolve in Mg at certain degree. Meanwhile, the other two metals will not form compounds or solid solutions with Mg. By comparing the substitutional energies of different layers, we find that all of the four metal impurities except In prefer to substitute Mg atoms in the inner layers rather than the outmost layer.

The interaction between transition metal impurities and Mg is dominated by the d levels of the metal impurities and the p levels of Mg [15]. When metals without partially filled 3d or 4d orbitals involved, we may discuss the charge transfer between metal impurities and Mg based on Pauling electronegativity. The Pauling electronegativity of Ti, Nb, and Al are 1.54, 1.60, and 1.61, while In is much stronger, with the value of 1.78. We have calculated the charge density difference of Mg (0001) surface structure alloyed with Ti/In (cf. Fig. 2). Here, $\rho_{\text{diff}} = \rho_{\text{Mg/M}} - \rho_{\text{Mg}} - \rho_{\text{M}}$, and $\rho_{\text{Mg/M}}$, ρ_{Mg} , ρ_{M} stand for the charge corresponding to the metal impurity doped Mg (0001) surface, the doped Mg (0001) surface with the impurity atom removed, and the free impurity atom, respectively. For Ti/In, the charges are transferred from the six nearest neighbor Mg atoms to the doped atoms since the doped impurities are of stronger electronegativity than that of Mg. According to Fig. 2, the

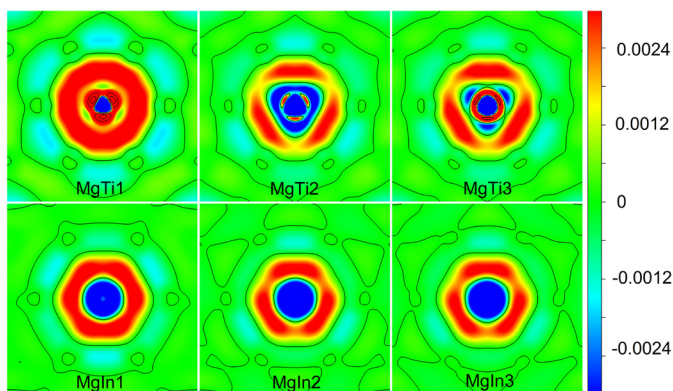


Fig. 2. (Color online.) Charge density difference (in unit of e/Bohr^3) of Mg (0001) surface structure alloyed with Ti and In. MgTi1, MgIn1, MgTi2, MgIn2, MgTi3, and MgIn3 represent Mg and In doped in the first, second, and third layers, respectively. Warm and cold colored areas indicate electron depletion and accumulation, respectively.

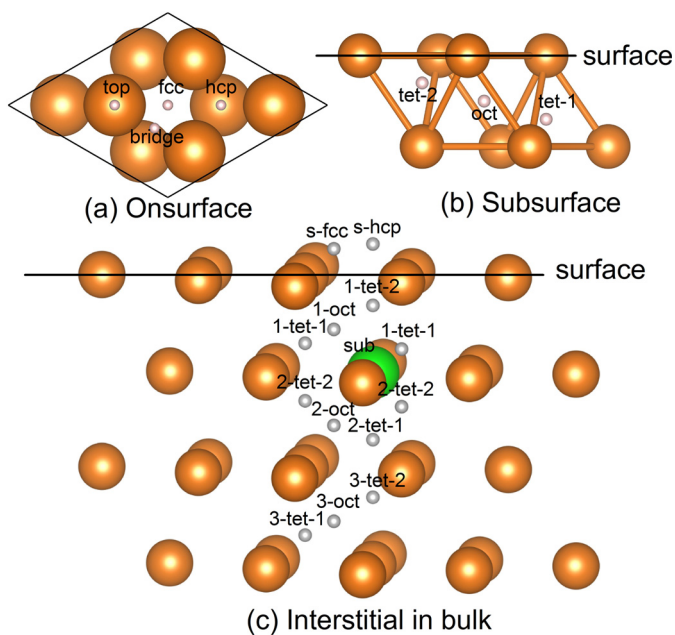


Fig. 3. (Color online.) Different high symmetry sites on or below Mg (0001) surface. (a) Four different adsorption sites for hydrogen atom on Mg (0001) surface; (b) Three different interstitial sites under the top layer of Mg (0001) surface; (c) Different interstitial sites in bulk Mg. The orange, white, and green balls denote Mg, hydrogen, and substitutional metal impurities, respectively.

accumulated electrons are mostly located around the center part of impurity metals, in particular for In cases, implying the stronger Pauli electronegativity of In than Ti.

According to the substitutional energy of different metal impurities doped Mg surfaces in different layers, we choose Mg surface with Ti, Nb, and Al doped in the second layer and In doped in the first and second layers since they are energetically favored. There are four possible adsorption sites for hydrogen atom on an ideal Mg (0001) surface, top, bridge, fcc hollow, and hcp hollow sites. Considering that hydrogen atoms diffuse into the interstitial site near the outmost layer of Mg (0001) surface, we know that three nonequivalent high symmetry sites are available, tetrahedral site-1 (tet-1), tetrahedral site-2 (tet-2), and octahedral site (oct), as illustrated in Fig. 3. Here, we select fcc hollow, hcp hollow, and three interstitial sites since they are more favorable for hydrogen atoms than the other sites.

The adsorption energy (E_{ad}) for hydrogen atom adsorbed on Mg (0001) surface is defined as:

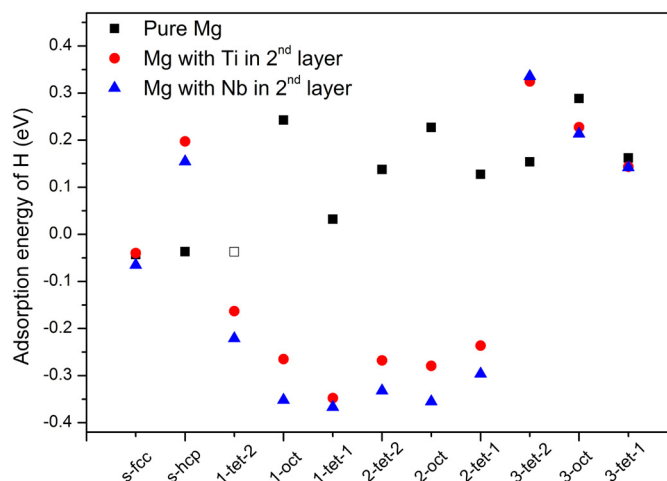


Fig. 4. (Color online.) The hydrogen adsorption energies of pure Mg (0001) surface and Ti or Nb doped Mg (0001) surface. The black empty squares represent hydrogen atom placed in the 1-tet-2 site, and consequently hydrogen atom will be pushed up to the surface hcp hollow site after a full structure relaxation.

$$E_{ad} = E_{H/\text{Mg}(0001)} - E_{\text{Mg}(0001)} - (1/2)E_{\text{H}_2}, \quad (2)$$

where $E_{H/\text{Mg}(0001)}$, $E_{\text{Mg}(0001)}$, and E_{H_2} are the energies of the slab with one hydrogen adsorbed on Mg surface, the Mg surface without hydrogen adsorbed, and an isolated hydrogen molecule, respectively. A positive value of E_{ad} indicates the adsorption configuration is unstable with respect to the hydrogen environment since the reaction between Mg surface and hydrogen is endothermic.

Our calculated results show that hydrogen atoms energetically prefer the fcc hollow sites on pure Mg (0001) surface, and particularly the nearest ones to the impurities when Ti and Nb are doped at the second layer. As for Al and In doped Mg (0001) surface, we find that the hydrogen atom placed on the nearest neighbor high symmetry sites around the doped atoms will be pushed to the second nearest neighbor high symmetry sites, i.e., the interaction between hydrogen and Al or In is repulsive. The difference of adsorption energy of hydrogen at fcc hollow site for pure, Ti doped, and Nb doped Mg (0001) surface is nearly negligible, but for hydrogen at the hcp hollow site, the difference is about 0.2 eV, as illustrated at s-fcc and s-hcp site in Fig. 4.

Subsequently, we calculate the formation energy of interstitial hydrogen sites around the doped atoms in the top three Mg layers. It is found that the hydrogen atom located in the interstitial site around the doped Al or In atoms will also be pushed far away from the doped atoms, but for pure, Ti doped, and Nb doped Mg (0001) surfaces, the hydrogen atom will stay at their original interstitial sites nearby the doped atoms. Therefore, we will continue to compare the formation energy of interstitial hydrogen at different high symmetry sites around the doped atoms in the top three layers of pure, Ti doped, and Nb doped Mg (0001) surfaces.

Fig. 4 shows the calculated formation energies of interstitial hydrogen at various sites corresponding to those in Fig. 3(c). We can come to a conclusion that the interaction between the hydrogen atom and Ti/Nb atom is remarkably strong. All the formation energies of interstitial hydrogen around Ti and Nb are negative with respect to the corresponding pure Mg interstitial sites. But when interstitial hydrogens is separated by a layer of Mg atoms with the doped Ti or Nb atom, such as the 3-oct site, the influence of Ti and Nb will degrade to be negligible. Thus, the doped impurities basically have an impact only on the formation of surrounding interstitial hydrogen atoms. We can find that the formation energy of pure Mg (0001) surface and Ti doped or Nb doped Mg (0001)

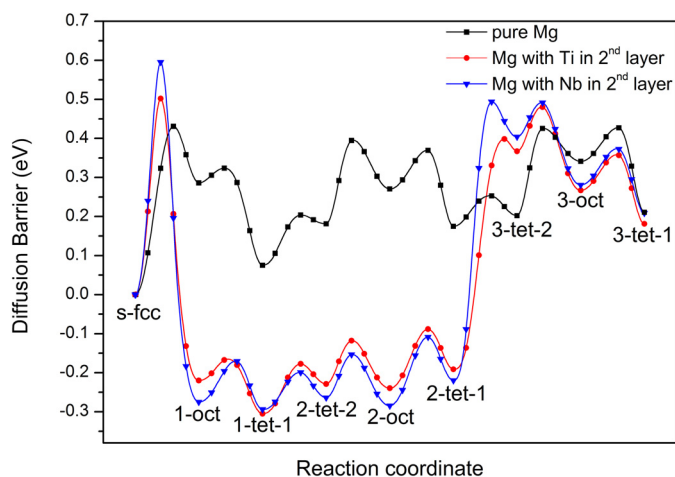


Fig. 5. (Color online.) Diffusion routes and barriers of hydrogen atom from surface fcc hollow site into the deeper tet-1 site below the third layers of pure, Ti doped, and Nb doped Mg (0001) surfaces.

surface is roughly equal when hydrogen adsorbed on the surface of Mg (0001) or in the third layer below the outmost layer.

The black empty square in Fig. 4 represents the hydrogen atom placed in the 1-tet-2 site between the first and second layers in pure Mg (0001) surface. It will migrate to the surface hcp hollow site after a full relaxation. While the corresponding H stays at 1-tet-2 site in Ti and Nb doped Mg surfaces. This is mainly attributed to the doping metal impurity and indicating that the interaction between hydrogen atoms and Ti/Nb atom is significantly strong.

According to above discussion, we know that the interaction between H and Nb/Ti is rather strong. However, Al and In have very weak interactions with H atom as H atoms are often pushed away from Al or In, although Al has a similar Pauling electronegativity of Nb (1.60 vs 1.61). We may summarize that H atoms has weak interaction with metals without partially filled 3d or 4d orbitals, while the interaction of transition metals are strongly related to their Pauling electronegativity, i.e., the larger electronegativity, the weaker interaction with H atom.

3.2. Diffusion of hydrogen

Following the above investigation of site preference of hydrogen atom, we investigate the diffusion of hydrogen atoms from surface into the bulk. For the diffusion of hydrogen from surface adsorbed site into subsurface interstitial site on impurity doped Mg (0001) surface, H at fcc or hcp hollow site on the surface and tetrahedral site-1 between the first and second layers are considered as the initial and final states respectively, and the octahedral site between them is expected to be an intermediate state according to the calculated adsorption configurations. For the sequentially diffusion of hydrogen from the shallower tetrahedral site-1 (between the first and second layer) into the deeper tetrahedral site-1 (below the second layer), the most probable pathway should follow the route: shallower tet-1 \rightarrow tet-2 \rightarrow oct \rightarrow deeper tet-1.

Fig. 5 shows the optimized MEP and their corresponding barriers for hydrogen diffusion from surface fcc hollow site into the deeper tet-1 site below the third layer for pure, Ti doped in the second layer, and Nb doped in the second layer of Mg (0001) surfaces, respectively. For the dissociated hydrogen atom initially adsorbed on Ti or Nb doped Mg (0001) surface, the fcc hollow site near the doped atoms is the initial state and the diffusion pathway follows the route: s-fcc \rightarrow 1-oct \rightarrow 1-tet-1 \rightarrow 2-tet-2 \rightarrow 2-oct \rightarrow 2-tet-1 \rightarrow 3-tet-2 \rightarrow 3-oct \rightarrow 3-tet-1, as shown in Fig. 3(c). Mean-

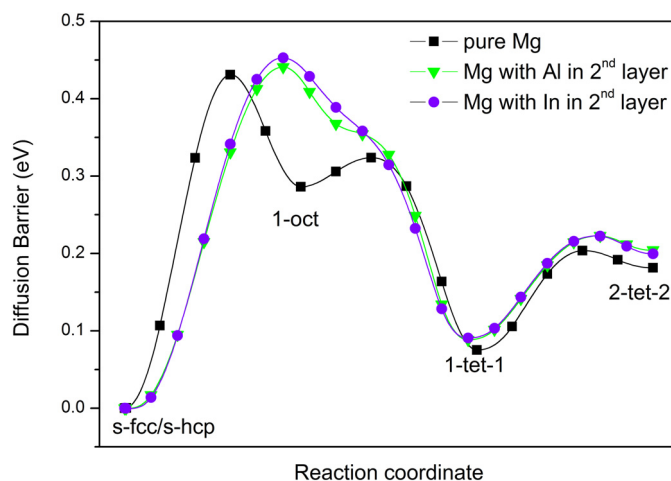


Fig. 6. (Color online.) Diffusion routes and barriers of hydrogen atom from surface fcc/hcp hollow site into the deeper 2-tet-2 site of pure, the second layer Al and In doped Mg (0001) surfaces.

while, we choose the same path for pure Mg (0001) surface as a reference.

As shown in Fig. 5, the diffusion barrier of H from surface fcc hollow site into subsurface 1-tet-1 site in pure Mg system is about 0.43 eV, which is in line with the theoretical result by Li et al. (0.45 eV) [34]. For Ti or Nb doped Mg systems, the corresponding diffusion barriers for adsorbed H are slightly higher to go through the first Mg layer. When hydrogen further diffuses from 1-tet-1 site into the deeper 2-tet-1 between the second and third Mg layers, the situation are completely different. We see from Fig. 5 that the diffusion barrier for H in pure Mg system is 0.32 eV, which is in line with the result by Xin et al. (0.31 eV) [22], nearly twice as large as that in Ti or Nb doped Mg systems. Finally, for the following diffusion of H down to the 3-tet-1 below the third Mg layer, the diffusion barrier has no remarkable change for pure Mg system. For Ti and Nb doped Mg systems, the diffusion barriers away from the doped atoms climb up to 0.60 eV and 0.71 eV respectively. It is understandable that the barrier will be small or negligible when H approaches to the impurities (such as Ti and Nb) with strong interaction with H, and a high barrier when H leaves the impurities.

It is obvious from our study that the hydrogen atom attempts to diffuse through the oct site to reduce the barriers, and hydrogen atoms diffuse easier around the doped Ti or Nb than in the pure Mg. With more Ti atoms spreading in Mg systems, the diffusion of hydrogen atom will become much easier, and this will be beneficial to the formation of trilayer H–Mg–H structure and its transition to Mg hydride.

Fig. 6 shows the optimized MEP and their corresponding barriers for hydrogen diffusion from surface fcc or hcp hollow site into the deeper 2-tet-2 site for pure, the second layer Al and In doped Mg (0001) surfaces. For the dissociated hydrogen atoms initially adsorbed on the second layer Al or In doped surfaces, the second nearest neighbor hcp hollow site near the doped atoms (not the top hcp hollow site of the doped atom) is the most preferable site and the diffusion pathway is expected to follow the route: s-hcp \rightarrow 1-tet-2 \rightarrow 1-oct \rightarrow 1-tet-1 \rightarrow 2-tet-2, as shown in Fig. 3(c). Meanwhile, we choose the similar path for pure Mg (0001) surface for comparison. As shown in Fig. 6, the oct site between 1-tet-2 and 1-tet-1 is not the intermediate state for the diffusion route of H around Al/In closely, due to the repulsive interaction between H and Al/In. As the hydrogen atom keeps away from the doped Al or In atoms, the practical diffusion routes and barriers in Al or In doped systems are basically no different from the pure Mg system.

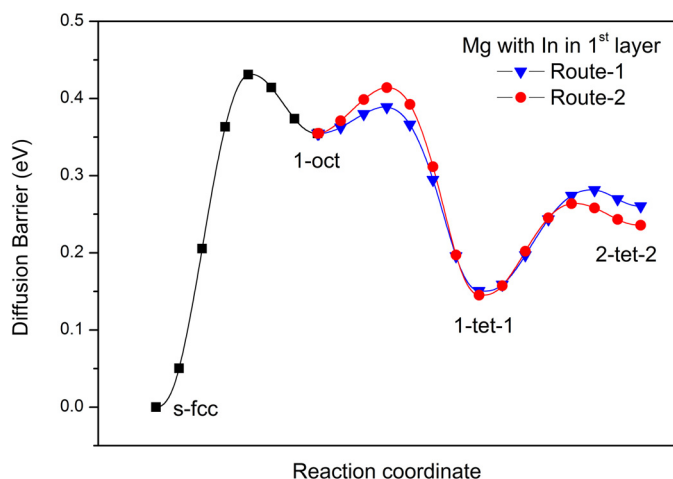


Fig. 7. (Color online.) Diffusion routes and barriers of hydrogen atom from surface fcc hollow site into the deeper 2-tet-2 site of In doped in the first layer of Mg (0001) surface.

Fig. 7 shows the optimized MEP and corresponding barriers for hydrogen diffusion from surface fcc hollow site into the deeper 2-tet-2 site for the first layer In doped surface. In this case, the second nearest neighbor fcc hollow site near the doped atom is the most preferable site at the beginning and the diffusion pathway should be the route: s-fcc \rightarrow 1-oct \rightarrow 1-tet-1 \rightarrow 2-tet-2, as shown in Fig. 3(c). As shown in Fig. 7, the octahedral site between 1-tet-2 and 1-tet-1 is the intermediate state for the diffusion. Since the interaction between hydrogen and Al/In is repulsive, Al and In have little impact to the practical diffusion of hydrogen atoms as they are far away from the impurities.

As a result, we conclude that the existence of the Al/In impurities, no matter in the first or second layer, the adsorbed hydrogen atom will keep away from the doped atom, and the diffusion will no much different from the pure Mg system. So the doped Al or In provides no obvious helps to the formation of trilayer H–Mg–H structure and its consequently transition to Mg hydride, though it might be beneficial to the hydrogen release from MgH₂.

4. Conclusions

In summary, we have performed a systematic theoretical investigation of hydrogen diffusion on four typical metal impurities (Ti, Nb, Al, and In) doped Mg (0001) surfaces. It is found that indium is miscible with Mg, while Al, Ti, and Nb prefer to the inner layers of bulk Mg. The interaction between H and Nb/Ti is rather strong, while the interaction between H and Al/In is weaker than that with Mg. Meanwhile, we reveal that the existence of the sub-surface Ti/Nb make hydrogen atom diffusion much easier into bulk Mg, and subsequently will be beneficial to the formation of trilayer H–Mg–H structure, which is crucial for the transition to Mg hydride. The doped Al or In atoms will, however, provide no clear helps in Mg hydrogenation.

Acknowledgements

This work is financially supported by NSFC (Grants 11574088, 51431001), the Foundation for Innovative Research Groups of the National Natural Science Foundation of China (Grant No. 51621001), and Natural Science Foundation of Guangdong Province of China (Grant No. 2016A030312011). The computer times at National Supercomputing Center in Guangzhou (NSCCGZ) is gratefully acknowledged.

References

- [1] P. Jena, *J. Phys. Chem. Lett.* 2 (3) (2011) 206–211.
- [2] H. Wang, H.J. Lin, W.T. Cai, L.Z. Ouyang, M. Zhu, *J. Alloys Compd.* 658 (2016) 280–300.
- [3] J. Yang, A. Sudik, C. Wolverton, D.J. Siegel, *Chem. Soc. Rev.* 39 (2) (2010) 656–675.
- [4] <https://energy.gov/eere/fuelcells/materials-based-hydrogen-storage>.
- [5] P. Selvam, B. Viswanathan, C.S. Swamy, V. Srinivasan, *Int. J. Hydrog. Energy* 11 (3) (1986) 169–192.
- [6] R.B. Schwarz, *Mater. Res. Soc. Bull.* 24 (11) (1999) 40–44.
- [7] J.H. Dai, Y. Song, B. Shi, R. Yang, *J. Phys. Chem. C* 117 (48) (2013) 25374–25380.
- [8] N.V. Mushnikov, A.E. Ermakov, M.A. Uimin, V.S. Gaviko, P.B. Terent'ev, A.V. Skripov, A.P. Tankeev, A.V. Soloninin, A.L. Buzlukov, *Phys. Met. Metallogr.* 102 (4) (2006) 421–431.
- [9] L. Schlapbach, A. Züttel, *Nature* 414 (6861) (2001) 353–358.
- [10] T. Vegge, *Phys. Rev. B* 70 (3) (2004) 035412.
- [11] M. Pozzo, D. Alfè, A. Amieiro, S. French, A. Pratt, *J. Chem. Phys.* 128 (9) (2008).
- [12] M. Pozzo, D. Alfè, *J. Phys. Condens. Matter* 21 (9) (2009) 095004.
- [13] G. Wu, J. Zhang, Y. Wu, Q. Li, K. Chou, X. Bao, *Appl. Surf. Sci.* 256 (1) (2009) 46–51.
- [14] H.P. Lei, C.Z. Wang, Y.X. Yao, Y.G. Wang, M. Hupalo, D. McDougall, M. Tringides, K.M. Ho, *J. Chem. Phys.* 139 (22) (2013).
- [15] M. Chen, X.B. Yang, J. Cui, J.J. Tang, L.Y. Gan, M. Zhu, Y.J. Zhao, *Int. J. Hydrog. Energy* 37 (1) (2012) 309–317.
- [16] J.H. Dai, Y. Song, R. Yang, *Int. J. Hydrog. Energy* 36 (20) (2011) 12939–12949.
- [17] H.C. Zhong, H. Wang, J.W. Liu, D.L. Sun, M. Zhu, *Scr. Mater.* 65 (4) (2011) 285–287.
- [18] Z. Luz, J. Genossar, P.S. Rudman, *J. Less-Common Met.* 73 (1) (1980) 113–118.
- [19] T. Jiang, L.-X. Sun, W.-X. Li, *Phys. Rev. B* 81 (3) (2010) 035416.
- [20] J.J. Tang, X.B. Yang, M. Chen, M. Zhu, Y.J. Zhao, *J. Phys. Chem. C* 116 (28) (2012) 14943–14949.
- [21] L. Ouyang, J. Tang, Y. Zhao, H. Wang, X. Yao, J. Liu, J. Zou, M. Zhu, *Sci. Rep.* 5 (2015) 10776.
- [22] J. Xin, J. Wang, Y. Du, L. Sun, B. Huang, *Int. J. Hydrog. Energy* 41 (5) (2016) 3508–3516.
- [23] G. Kresse, J. Furthmüller, *Phys. Rev. B* 54 (16) (1996) 11169.
- [24] G. Kresse, J. Furthmüller, *Comput. Mater. Sci.* 6 (1) (1996) 15–50.
- [25] P.E. Blöchl, *Phys. Rev. B* 50 (24) (1994) 17953–17979.
- [26] G. Kresse, D. Joubert, *Phys. Rev. B* 59 (3) (1999) 1758–1775.
- [27] J.P. Perdew, K. Burke, M. Ernzerhof, *Phys. Rev. Lett.* 78 (7) (1997) 1396.
- [28] M. Chen, Z.Z. Cai, X.B. Yang, M. Zhu, Y.J. Zhao, *Surf. Sci.* 606 (13–14) (2012) L45–L49.
- [29] C. Kittel, *Introduction to Solid State Physics*, 8th ed., Wiley, New York, 2005.
- [30] T. Jiang, L.X. Sun, W.X. Li, *Phys. Rev. B* 81 (3) (2010).
- [31] H.J. Monkhorst, J.D. Pack, *Phys. Rev. B* 13 (12) (1976) 5188–5192.
- [32] G. Henkelman, B.P. Uberuaga, H. Jónsson, *J. Chem. Phys.* 113 (22) (2000) 9901–9904.
- [33] S. Banerjee, C.G.S. Pillai, C. Majumder, *J. Chem. Phys.* 129 (17) (2008) 174703.
- [34] Y. Li, P. Zhang, B. Sun, Y. Yang, Y. Wei, *J. Chem. Phys.* 131 (3) (2009) 034706.